J. Mol. Biol. (1996) **260**, 649–663

JMB

Co-variation of tRNA Abundance and Codon Usage in *Escherichia coli* at Different Growth Rates

Hengjiang Dong, Lars Nilsson and Charles G. Kurland*

Department of Molecular Biology, Biomedical Centre Box 590, Uppsala, S-751 24 Sweden

**Corresponding author*

We have used two-dimensional polyacrylamide gel electrophoresis to fractionate tRNAs from *Escherichia coli*. A sufficiently high degree of resolution was obtained for 44 out of 46 tRNA species in *E. coli* to be resolved into individual electrophoretic components. These isolated components were identified by hybridization to tRNA-specific oligonucleotide probes. Systematic measurements of the abundance of each individual tRNA isoacceptor in *E. coli*, grown at rates varying from 0.4 to 2.5 doublings per hour, were made with the aid of this electrophoretic protocol. We find that there is a biased distribution of the tRNA abundance at all growth rates, and that this can be roughly correlated with the values of codon frequencies in the mRNA pools calculated for bacteria growing at different rates. The tRNA species cognate to abundant codons increase in concentration as the growth rate increases but not as dramatically as might be anticipated. The levels of most of the tRNA isoacceptors cognate to less abundant codons remain unchanged with increasing growth rates. The result of these changes in tRNA abundance is that the relative increase in the amounts of major tRNA species in the bacteria growing at the fastest growth rates is more modest than previous estimates from this laboratory suggested. Furthermore, a systematic error in previous estimates of ribosomal RNA content of the bacteria has been detected. This will account for the quantitative discrepancies between the previous and the present data for tRNA abundance.

Keywords: Escherichia coli; growth rate; codon usage; tRNA abundance; synonymous codon

Introduction

Escherichia coli has 79 tRNA genes coding for 46 different amino acid acceptor species (Komine *et al*., 1990). However, the distribution of these tRNA species is not uniform. Thus, the tRNAs present at relatively higher concentrations (major tRNAs) are those cognate to the preferred codons of the genes coding the highly expressed proteins of rapidly growing bacteria (Ikemura, 1981; Ikemura & Ozeki, 1983). This arrangement of biased codon usage and matching tRNA abundance has been viewed as an optimal arrangement for bacteria to maximize the efficiency of translation and, consequently, to maximize their growth rates in rich media (Ehrenberg & Kurland, 1984; Kurland, 1993).

Quantitative estimates of two initiator and 18 elongator tRNA species extracted from bacteria growing at different rates suggested that the abundance of most tRNA isoacceptors changes in ways that are consistent with the growth optimization hypothesis. In particular, major tRNA species cognate to preferred codons seem to increase in abundance while most of the minor tRNA species cognate to rare codons decrease in abundance as the growth rates of the bacteria increase (Emilsson & Kurland, 1990; Emilsson *et al*., 1993). Surprisingly, the abundance of four of the 11 minor tRNA species that were quantified seemed to vary in an anomalous way: they increase in amounts relative to ribosomal RNA when the growth rate is increased (Emilsson & Kurland, 1990; Emilsson *et al*., 1993).

The previous data from our laboratory describing tRNA abundance (Emilsson & Kurland, 1990; Emilsson *et al*., 1993) were obtained by adapting a quantitative Northern blot protocol. The tRNA estimates according to this procedure are dependent on extrapolations from a titration curve

Abbreviation used: TBE, Tris-HCl/boric acid/EDTA.

0022–2836/96/300649–15 $18.00/0

constructed from hybridization reactions between individual purified tRNAs and the corresponding oligonucleotide probes. The data described in the present study were obtained by a simpler protocol in which the quantities of nearly all of the tRNA species are estimated from a single two-dimensional electrophoretic gel. In order to obviate the problem of partial loss of tRNA species during the extraction of gel samples, we have relied on double-labelling procedures to measure the amounts of the individual tRNA species.

We have employed this two-dimensional gel system for a systematic study of the abundance of all the tRNAs in *E. coli* grown at rates varying from 0.4 to 2.5 doublings per hour. As before, we find that there is a biased distribution of the tRNA composition for cells grown at each of the growth rates that were assayed, and that the degree of bias increases at higher growth rates. Here, the tRNAs present at relatively higher concentrations at the lowest growth rates increase in abundance with increasing growth rates. In contrast, the abundance of the tRNAs present in lower amounts at the lowest growth rates remains unchanged, or nearly so, as growth rates are increased.

These data are in general agreement with previous reports (Emilsson & Kurland, 1990; Emilsson *et al*., 1993), but they differ significantly in the magnitude of the tRNA response to growth rate variations. The earlier data suggest that there are five- to tenfold increases in the abundance of the major tRNA species as growth rates are increased from 0.5 to 2.1 doublings per hour (Emilsson & Kurland, 1990; Emilsson *et al*., 1993). In contrast, we find now that there is at most a twofold increase for the major tRNA isoacceptors as the growth rates are varied from 0.4 to 2.5 doublings per hour. There are a number of sources for these discrepancies, which are discussed in detail below, but the primary one seems to be a systematic underestimation of ribosomal RNA quantities that distorted the previous calculations.

Finally, we have used the data of Pedersen *et al*. (1978) as well as that from the protein database of VanBogelen *et al*. (1992), together with coding sequences from Genbank, to calculate the codon frequencies of the *E. coli* mRNA pools being translated at different growth rates. These have been compared with the distributions of tRNAs present in the bacteria at the same growth rates. This comparison reveals a systematic correlation between the biased distribution of tRNA species and the biased usage of the corresponding codons. However, the form of this correlation is not consistent with the simplest theoretical expectations.

Results

A two-dimensional polyacrylamide gel system

In order to obtain a systematic measurement of the cellular concentration for all tRNA species in *E. coli*, we used two-dimensional polyacrylamide gel electrophoresis to fractionate the tRNAs. Here, the first dimension consisted of a 10% (w/v) polyacrylamide gel and the second dimension a 20% (w/v) polyacrylamide gel. By varying the amount of urea used in the gel from 7 M in the first dimension to 4 M in the second dimension, we have obtained a high-degree of resolution such that the tRNAs and 4.5 S RNA from *E. coli* are fractionated into 50 electrophoretic components (Figure 1).

The identity of individual electrophoretic spots was determined using oligonucleotide probes that are complementary to specific regions of each tRNA isoacceptor in *E. coli* as described in Materials and Methods. Accordingly, we have identified each electrophoretic component on our two-dimensional gels with only one exception, which is spot 50. The RNA in spot 50 fails to hybridize with any of the specific oligonucleotide probes that we used here (Table 1). It remains to be determined whether or not the spot 50 RNA is a previously unidentified tRNA isoacceptor (Komine *et al*., 1990).

Data in Figure 1 and Table 2 show that most of the tRNA species correspond to one electrophoretic component except or $tRNA_4^{Leu}$, $tRNA_2^{Arg}$, $tRNA_3^{Gly}$ and $tRNA_2^{Ala}$. Each of these was identified in two electrophoretic components. In addition, $tRNA_1^{Ile}$ and $tRNA_2^{Ile}$ comigrate as one component as do $tRNA_1^{Gly}$ and $tRNA_2^{Gly}$ (Figure 1 and Table 2).

Growth rate-dependent variations of tRNA abundance

The quantification of individual tRNA species involves two sorts of experiments. In one experiment, we make measurements of the amounts of individual tRNA species accumulated in cells grown at the slowest rate (e.g. 0.4 doubling/hour) by labelling an exponentially growing culture with [U-^{14}C]uridine for five hours (two generations) as described in Materials and Methods. The molar ratio of each individual tRNA to $tRNA_1^{Leu}$ was calculated by normalizing the amount of radioactivity in the respective tRNA spot to that in the spot of $tRNA_1^{Leu}$, after correction for the small differences in the number of uridines that each contains.

The relative changes in tRNA content were measured using a double-labelling experiment. Exponentially growing cells in the five media were each uniformly labelled with [5,6-^{3}H]uridine in the presence of carrier uridine for two generations (Materials and Methods). In addition, a separate logarithmic culture of W1485 in a low-phosphate MOPS/acetate medium was uniformly labelled with [^{32}P]orthophosphate for five hours to provide a reference culture labelled at a growth rate of 0.4 doubling/hour. After the RNA was fractionated on two-dimensional gels, the isotope ratio of $^3H/^{32}P$ in each individual tRNA spot was measured and normalized to the isotope ratio in the spot corresponding to $tRNA_1^{Leu}$. These normalized values were used for calculations of the molar ratio of individual tRNA to $tRNA_1^{Leu}$ for the cell at different

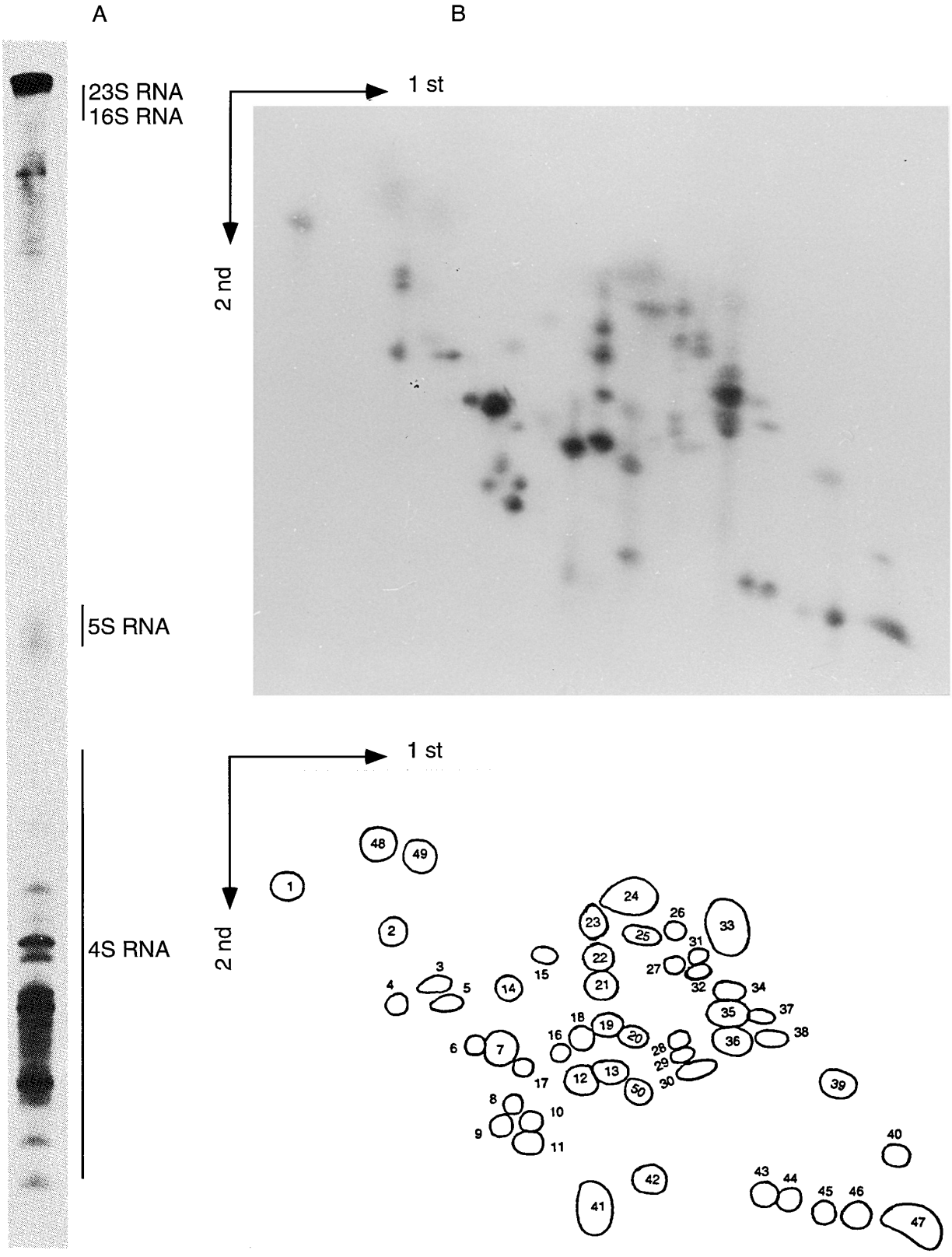

Figure 1. Two-dimensional separation of all the tRNAs of *E. coli*. A 5 µg sample of total RNA isolated from ^{32}P-labelled cells in low phosphate MOPS medium was applied to the first-dimensional polyacrylamide gel. Subsequent electrophoresis of the first and the second-dimensional gels was carried out as described in the text. The autoradiograms of the first (A) and the second (B)-dimensional polyacrylamide gels are shown here. The spot numbers of individual electrophoretic components are shown in the schematic diagram (Figure 1b) and their corresponding tRNA identities are listed in Table 2.

Table 1. The synthetic DNA oligonucleotides specific for the respective tRNA isoacceptors, 4.5 S RNA and 16 S rRNA of *Escherichia coli*

tRNA	Oligonucleotide sequence (5'–3')	Remark
Ala1B	CAG ACC TCC TGC GTG CAA A	This work
Ala2	CTG ACC TCT TGC ATG CCA T	This work
Arg2	CCT CCG ACC GCT CGG TTC G	Emilsson *et al.* (1993)
Arg3	CCT GAG ACC TCT GCC TCC GGA	Emilsson *et al.* (1993)
Arg4	CCT GCG GCC CAC GAC TTA G	Emilsson *et al.* (1993)
Arg5	CCT GCA ATT AGC CCT TAG G	Emilsson *et al.* (1993)
Asn	CCA GTG ACA TAC GGA TTA ACA	This work
Asp1	CCC GCG ACC CCC TGC GTG ACA	This work
Cys	GGA CTA GAC GGA TTT GCA A	This work
Gln1	AGG GAA TGC CGG TAT CAA A	This work
Gln2	TCG GAA TGC CGG AAT CAG A	This work
Glu2	CCC CTG TTA CCG CCG TG	Emilsson *et al.* (1993)
Gly1	CCC TCG TAT AGA GCT TGG GAA	Emilsson *et al.* (1993)
Gly2	CCC GCA TCA TCA GCT TGG AAG GC	Emilsson *et al.* (1993)
Gly3	CTC GCG ACC CCG ACC TTG GCA AG	Emilsson *et al.* (1993)
His	CAC GAC AAC TGG AAT CAC	This work
Ile1	ACC GAC CTC ACC CTT ATC AG	This work
Ile2	AGC GAC CAA GCG ATT ATG AG	This work
Leu1	CCC CCA CGT CCG TAA GGA CA	Emilsson & Kurland (1990)
Leu2	CCC GTA AGC CCT ATT GGG CA	Emilsson & Kurland (1990)
Leu3	CAC CTT GCG GCG CCA GAA	Emilsson & Kurland (1990)
Leu4	CCG GCA CGT ATT TCT ACG G	Emilsson & Kurland (1990)
Leu5	CCC GCACAG CGC GAA CGC CG	Emilsson & Kurland (1990)
Lys	CCT GCG ACC AAT TGA TTA AA	This work
Met f1	CGG GTT ATG AGC CCG ACG A	Emilsson & Kurland (1990)
Met f2	CGG GTT ATG AGC CCG ACG A	Emilsson & Kurland (1990)
Met m	CCT GTG ACC CCA TCA TTA TGA G	Emilsson & Kurland (1990)
Phe	TGC TCT ACC GAC TGA GCT A	Emilsson & Kurland (1990)
Pro1	CCT CCG ACC CCT TCG TCC CG	Emilsson *et al.* (1993)
Pro2	CCT CCG ACC CCC GAC ACC CCA T	Emilsson *et al.* (1993)
Pro3	CCT CCG ACC CAC TGG TCC CAA A	Emilsson *et al.* (1993)
Sel-Cys	TGC CCG GGA CCG CTG GCG GCC CCA A	This work
Ser1	AAC CCT TTC GGG TCG CCG GTT TTC	Emilsson & Nilsson (1995)
Ser2	GTA GAG TTG CCC CTA CTC CGG T	Emilsson & Nilsson (1995)
Ser3	CCC CGG ATG CAG CTT TTG ACC	Emilsson & Nilsson (1995)
Ser5	ATA CGT TGC CGT ATA CAC AC	Emilsson & Nilsson (1995)
Thr1	CTG GGG ACC CCA CCC CT	Emilsson & Nilsson (1995)
Thr2	CCT ACG ACC TTC GCA TT	Emilsson & Nilsson (1995)
Thr3	CTG CCG ACC TCA CCC TT	Emilsson & Nilsson (1995)
Thr4	CTG GTG ACC TAC TGA TT	Emilsson & Nilsson (1995)
Trp	CCC AAC ACC CGG TTT TGG	This work
Tyr1	TTC GAA GTC GAT GAC GGC AGA	This work
Tyr2	TTC GAA GTC TGT GAC GGC AGA	This work
Val1	CGC CGA CCC CCT CCT TGT AAG	This work
Val2A	CAC CGA CCC CCA CCA TGT CAA	This work
Val2B	CAA CGA CCC CCA CCA TGT CAA	This work
4.5 S RNA	TGC CAG CTA CAT CCC GGC ACA CGC GTC AT	This work
16 S rRNA	TGC GCT TTA CGC CCA GTA	Emilsson & Kurland (1990)

growth rates. In the following experiment, we quantified the molar ratio of $tRNA_1^{Leu}$ to ribosome in cells so that ribosome-normalized variations for all of the tRNA isoacceptors with growth rate could be calculated.

The molar ratio of ribosome $tRNA_1^{Leu}$ to ribosome

The molar ratio of $tRNA_1^{Leu}$ to 16 S rRNA in the cell at different growth rates was measured in total RNA that was isolated from cells at each of the five growth rates and fractionated on a denaturing agarose/formaldehyde gel (Dong *et al*., 1995). In addition, titrations with known amounts of pure ribosomal RNA and pure $tRNA_1^{Leu}$ were carried out in the same gels to provide standard curves from which to extrapolate the values for the experimental samples. After trans-blotting, the filter was hybridized with two oligonucleotide probes: one specific for 16 S rRNA and the other specific for $tRNA_1^{Leu}$.

The amounts of hybridizable probe (expressed as counts/minute) recovered on the filter is linearly proportional to the amounts of the standard RNA material applied in our titration experiments within the range of 1 to 5 μg for 16 S rRNA and 30 to 200 ng for $tRNA_1^{Leu}$, respectively (Figure 2). Care has been taken to ensure that the amounts of total RNA applied to the agarose gels were within the linear response region in the titration curves (Figure 2A and B). Then, the amounts of $tRNA_1^{Leu}$ and of 16 S

Table 2. *E. coli* tRNAs and the codon recognition pattern

tRNA	Anticodon (5'–3')	Codon recognition (5'–3')	Spot number on 2D gel	No. of molecules per cell	Fraction of tRNA out of total tRNA (%)
Ala1B	UGC	GCU, GCA, GCG	46	3250(±223)	5.04
Ala2	GGC	GCC	28, 29	617(±64)	0.95
Arg2	ACG	CGU, CGC, CGA	21, 22	4752(±440)	7.37
Arg3	CCG	CGG	37	639(±63)	0.99
Arg4	UCU	AGA	17	867(±160)	1.34
Arg5	CCU	AGG	16	420(±69)	0.65
Asn	GUU	AAC, AAU	42	1193(±127)	1.85
Asp1	GUC	GAC, GAU	12	2396(±346)	3.72
Cys	GCA	UGC, UGU	25	1587(±126)	2.46
Gln1	UUG	CAA	31	764(±66)	1.18
Gln2	CUG	CAG	32	881(±94)	1.36
Glu2	UUC	GAA, GAG	47	4717(±411)	7.32
Gly1[a]	CCC	GGG	24		
Gly2	UCC	GGA, GGG	24	2137(±320)	3.31
Gly3	GCC	GGC, GGU	34, 35	4359(±378)	6.76
His	GUG	CAC, CAU	26	639(±95)	0.99
Ile1	GAU	AUC, AUU	13	3474(±94)	5.39
Ile2[a]	CAU	AUA	13		
Leu1	CAG	CUG	7	4470(±346)	6.94
Leu2	GAG	CUC, CUU	5	943(±97)	1.46
Leu3	UAG	CUA, CUG	23	666(±94)	1.03
Leu4	CAA	UUG	10, 11	1913(±190)	2.97
Leu5	UAA	UUA, UUG	2	1031(±117)	1.60
Lys	UUU	AAA, AAG	44	1924(±185)	2.97
Met f1	CAU	AUG	38	1211(±191)	1.88
Met f2	CAU	AUG	40	715(±107)	1.11
Met m	CAU	AUG	41	706(±96)	1.09
Phe	GAA	UUC, UUU	33	1037(±162)	1.60
Pro1	CGG	CCG	43	900(±150)	1.38
Pro2	GGG	CCC, CCU	27	720(±125)	1.11
Pro3	UGG	CCA, CCU, CCG	45	581(±95)	0.90
Sec	UCA	UGA	15	219(±73)	0.34
Ser1	UGA	UCA, UCU, UCG	4	1296(±94)	2.01
Ser2	CGA	UCG	3	344(±62)	0.53
Ser3	GCU	AGC, AGU	1	1408(±126)	2.18
Ser5	GGA	UCC, UCU	9	764(±127)	1.18
Thr1	GGU	ACC, ACU	14	104(±34)	0.16
Thr2	CGU	ACG	18	541(±94)	0.84
Thr3	GGU	ACC, ACU	19	1095(±62)	1.70
Thr4	UGU	ACA, ACU, ACG	8	916(±64)	1.42
Trp	CCA	UGG	39	943(±162)	1.46
Tyr1	GUA	UAC, UAU	49	769(±95)	1.19
Tyr2	GUA	UAC, UAU	48	1261(±126)	1.95
Val1	UAG	GUA, GUG, GUU	36	3840(±218)	5.96
Val2A	GAC	GUC, GUU	30	630(±98)	0.97
Val2B	GAC	GUC, GUU	20	635(±95)	0.98
4.5 S RNA			6	416(±63)	0.64

The assignment of individual tRNA identities to the electrophoretic components in the two-dimensional gel (Figure 1B) is represented by spot numbers. The number of tRNA molecules per cell and the fraction of tRNA out of total tRNA population in *E. coli* grown at 0.4 doubling per hour are shown here, as described in the text. ± stands for the standard deviations calculated from six independent measurements for each individual tRNA isoacceptor. The data on tRNA–codon recognition patterns were obtained from Komine *et al*. (1990), Björk (1995), Ikemura & Ozeki (1983), Ikemura (1985), Garcia *et al*. (1986) and Saxena & Walker (1992).

[a] The tRNA isoacceptors Gly1 and Gly2 are treated collectively as is the data for Ile1 and Ile2.

rRNA in each sample were determined on the basis of these quantitative titration curves; these data are summarized in Figure 2C. We find that there is a 50% reduction in the molar amount of $tRNA_1^{Leu}$ normalized to that of 16 S rRNA in the cell as growth rates increase from 0.4 to 2.5 doublings per hour (Figure 2C).

Next, we combined the data for the growth rate-dependent variations of tRNAs normalized to $tRNA_1^{Leu}$ and those of the $tRNA_1^{Leu}$ normalized to ribosomal RNA (rRNA) to calculate the molar ratio of individual tRNA isoacceptors to ribosome for cells grown at different rates varying from 0.4 to 2.5 doublings per hour. These data are summarized in Table 3. All tRNA species decrease to a greater or lesser extent in abundance relative to ribosomes with increasing growth rates. The calculated total tRNA/rRNA ratio also decreases about 50% as growth rates are increased from 0.4 to 2.5 doublings per hour (Figure 3).

Growth rate-dependent variations of total tRNA content

The amount of total tRNA relative to total ribosomal RNA was determined by comparing the

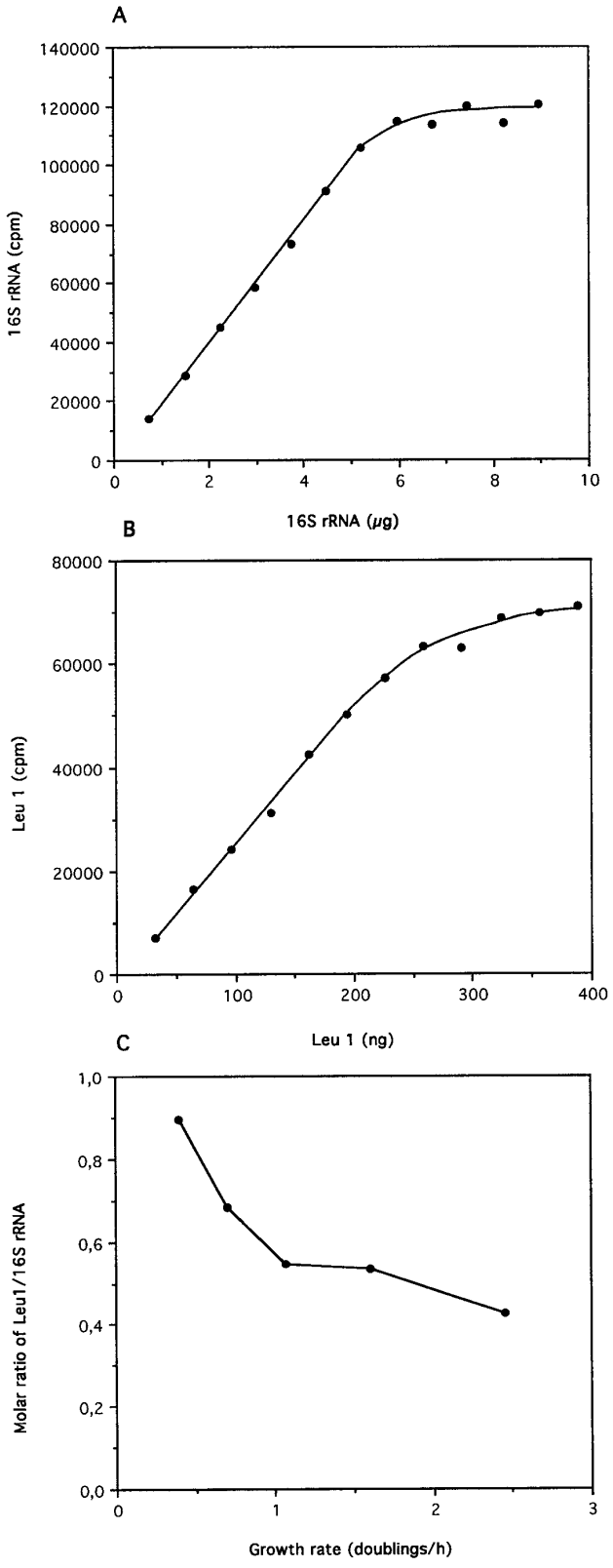

Figure 2. The molar ratio of $tRNA_1^{Leu}$/16 S rRNA at different growth rates. C, Determination of the molar ratio of $tRNA_1^{Leu}$/16 S rRNA as a function of growth rate is as described in Materials and Methods using a quantitative Northern blotting protocol with: A, titrations of the pure 16 S rRNA; and B, the pure $tRNA_1^{Leu}$ material.

amounts of radioactive [5,6-^{3}H]uridine incorporated into total RNA and that into the total ribosomal RNA in a steady-state labelling experiment as described in Materials and Methods. The data summarized in Figure 4 show that there is close to a 50% reduction in the mass ratio of total tRNA/rRNA as growth rates are increased from 0.4 to 2.5 doublings per hour. This is in good agreement with the calculations based on data obtained for the individual tRNAs in the two-dimensional gel system (Figure 3).

Correlation between the codon usage and the abundance of cognate tRNA

We have computed the codon frequencies for all 61 sense codons at different growth rates using the data of Pedersen *et al*. (1978) and that of VanBogelen *et al*. (1992) as well as the protein coding sequences from Genbank. Here, we have assumed that the relative ratios of mRNA species are proportional to the relative ratios of the protein species observed at each growth rate. The calculations are summarized in Table 4.

Evidently there is a biased usage of codons at all growth rates studied. The relative frequency of usage for some of the abundant codons increases somewhat while for others the frequencies remain relatively constant when the growth rate increases. The relative frequency of usage for rare codons decreases with increasing growth rate. None of the changes in the frequency of usage for particular codons is dramatic; they correspond to a twofold increase at most (Table 4). There is a clear correlation between the abundance of individual tRNA isoacceptors and the frequency of usage for the corresponding codons at each of the five growth rates that were studied. It is evident that the distributions are somewhat more skewed at the highest growth rates than they are at the lowest (Figure 5).

tRNA abundance and gene dose

It has been suggested previously that the amounts of 26 tRNA species accumulated in bacteria is correlated with the copy numbers of their corresponding genes (Ikemura, 1981). In order to determine whether this correlation can be extended to all of the tRNAs of *E. coli*, we plotted the cellular concentration of each individual tRNA isoacceptor as a function of the number of copies of their genes, according to the data of Komine *et al*. (1990). We too observe a clear tendency for the concentrations of individual tRNA species to increase as their gene dose increases (Figure 6). However, we also observe a very marked dispersion for the concentrations of tRNA species that are coded by only one gene. This spread may be explained, in part, by our observation that the measurements of the amounts of the least abundant tRNA species are associated with the greatest experimental uncertainties (Table 2). In addition, it

Table 3. The molar ratio of tRNA/ribosome at different growth rates (doublings/hour)

tRNA	0.4	0.7	1.07	1.6	2.5
Ala1B	0.65	0.54	0.46	0.44	0.40
Ala2	0.12	0.10	0.08	0.08	0.07
Arg2	0.95	0.67	0.50	0.60	0.49
Arg3	0.13	0.12	0.05	0.06	0.04
Arg4	0.17	0.11	0.09	0.08	0.07
Arg5	0.08	0.07	0.05	0.06	0.04
Asn	0.24	0.18	0.14	0.15	0.14
Asp1	0.48	0.37	0.27	0.30	0.29
Cys	0.32	0.22	0.17	0.18	0.14
Gln1	0.15	0.12	0.12	0.08	0.08
Gln2	0.18	0.14	0.11	0.13	0.12
Glu2	0.94	0.71	0.54	0.61	0.56
Gly1 + 2	0.43	0.33	0.25	0.28	0.21
Gly3	0.87	0.70	0.55	0.50	0.48
His	0.13	0.10	0.09	0.08	0.08
Ile1 + 2	0.69	0.54	0.43	0.47	0.47
Leu1	0.89	0.68	0.55	0.54	0.42
Leu2	0.19	0.16	0.13	0.12	0.11
Leu3	0.13	0.11	0.09	0.08	0.06
Leu4	0.38	0.29	0.23	0.24	0.18
Leu5	0.23	0.16	0.13	0.09	0.07
Lys	0.38	0.31	0.24	0.22	0.20
Met f1	0.24	0.22	0.19	0.16	0.19
Met f2	0.14	0.10	0.08	0.09	0.07
Met m	0.14	0.12	0.09	0.10	0.09
Phe	0.21	0.17	0.14	0.12	0.10
Pro1	0.18	0.11	0.11	0.07	0.05
Pro2	0.14	0.12	0.07	0.10	0.07
Pro3	0.12	0.09	0.07	0.06	0.05
Sel-Cys	0.04	0.04	0.03	0.03	0.02
Ser1	0.26	0.25	0.18	0.17	0.14
Ser2	0.07	0.05	0.04	0.03	0.03
Ser3	0.28	0.20	0.15	0.14	0.11
Ser5	0.15	0.12	0.09	0.09	0.08
Thr1	0.02	0.02	0.02	0.01	0.01
Thr2	0.11	0.09	0.07	0.07	0.06
Thr3	0.22	0.17	0.13	0.12	0.11
Thr4	0.18	0.14	0.11	0.12	0.13
Trp	0.19	0.13	0.11	0.10	0.10
Tyr1	0.15	0.11	0.09	0.12	0.08
Tyr2	0.25	0.18	0.12	0.13	0.10
Val1	0.77	0.55	0.36	0.48	0.39
Val2A	0.13	0.09	0.08	0.07	0.05
Val2B	0.13	0.11	0.09	0.09	0.08
4.5 S RNA	0.08	0.07	0.06	0.05	0.05

The molar ratio of each individual tRNA to $tRNA_1^{Leu}$ was determined from two-dimensional gels as described in the text. The molar ratio of $tRNA_1^{Leu}$ to ribosomes was quantified using a titrational Northern blotting procedure. The molar ratios of individual tRNA isoacceptors to ribosomes at different growth rates were calculated from these data.

may reflect a greater variation of the abundances of the minor tRNA species than is evident for major tRNA species. Comparable results were obtained for bacteria grown at each of the five growth rates.

Discussion

We have characterized the growth rate-dependent variations in abundance of all tRNA species in *E. coli* using measurements of recovery from two-dimensional polyacrylamide gels. These 46 tRNA isoacceptors correspond to the 41 unique anticodons that translate all 61 sense codons in bacteria (Komine *et al*., 1990). In addition, the 4.5 S RNA, was resolved in our electrophoretic fractionations and the growth rate-dependent variations of its abundance were also determined. We note in passing that the 4.5 S RNA varies in amount relative to ribosomes very much like a tRNA and not at all like a ribosomal RNA.

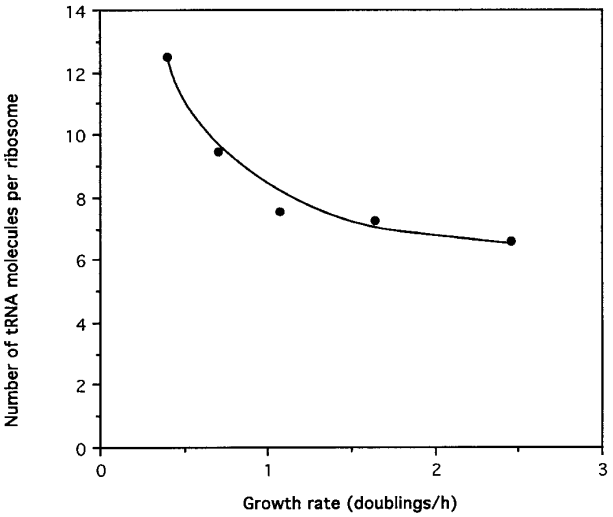

Figure 3. The molar ratio of total tRNA/ribosome at different growth rates. Data are calculated from Table 3.

Comparisons with previous work

The present data concerning the relative abundance of tRNA species in bacteria grown at the slowest rates are in reasonable agreement with those of Ikemura (1981), who quantified 26 tRNA species in *E. coli*, and with those of Emilsson &

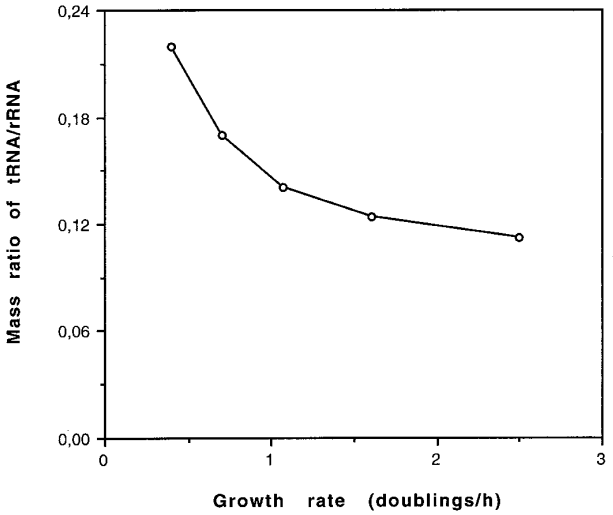

Figure 4. The mass ratio of total tRNA/total rRNA at different growth rates. The mass of total tRNA and that of total ribosomal RNA (23 S + 16 S + 5 S rRNA) are determined by measuring the amount of [5,6-^{3}H]uridine incorporated into the respective RNA materials in a steady-state labelling experiment (see Materials and Methods). The calculated mass ratio between total tRNA and total rRNA is plotted as a function of growth rate.

Table 4. The frequency of codon usage (1×10^{-3}) as different growth rates (doublings / hour)

Codon 5'–3'	Cognate tRNA	0.4	0.7	1.07	1.6	2.5
GGG	Gly1, 2	4.81	4.26	3.57	2.79	2.36
GGA	Gly2	2.71	2.49	2.21	1.79	1.26
GGU	Gly3	38.29	39.18	40.49	42.27	45.55
GGC	Gly3	35.62	35.58	35.54	35.49	34.17
GAG	Glu2	16.57	16.78	17.04	17.31	16.97
GAA	Glu2	53.10	53.94	55.10	56.68	57.86
GAU	Asp1	24.25	23.43	22.40	21.08	19.27
GAC	Asp1	28.72	29.65	30.93	32.35	33.74
GUG	Val1	21.40	20.34	18.93	17.74	14.98
GUA	Val1	15.87	17.05	18.65	19.95	22.31
GUU	Val1, 2A, 2B	31.31	33.10	35.63	38.14	43.18
GUC	Val2A, 2B	11.25	10.58	9.71	8.86	7.67
GCG	Ala1B	30.33	29.55	28.45	27.29	24.11
GCA	Ala1B	22.13	22.19	22.38	23.07	24.87
GCU	Ala1B	28.85	30.31	32.41	34.79	39.49
GCC	Ala2	19.80	18.50	16.81	14.67	11.81
AGG	Arg5	0.09	0.07	0.05	0.03	0.03
AGA	Arg4	1.12	0.99	0.84	0.65	0.63
AGU	Ser3	3.99	3.55	3.01	2.38	2.19
AGC	Ser3	11.97	11.40	10.69	9.88	9.31
AAG	Lys	12.08	12.76	13.74	14.89	17.22
AAA	Lys	44.43	46.41	49.07	51.99	55.01
AAU	Asn	9.79	8.88	7.79	6.43	5.61
AAC	Asn	27.95	28.22	28.64	29.02	29.21
AUG	Met m	22.37	22.36	22.34	22.30	21.67
AUA	Ile2	0.93	0.85	0.75	0.61	0.52
AUU	Ile1	21.38	20.45	19.26	17.72	15.79
AUC	Ile1	36.68	37.72	39.15	41.38	43.86
ACG	Thr2, 4	7.53	6.95	6.21	5.20	4.17
ACA	Thr4	3.48	3.25	2.99	2.63	2.61
ACU	Thr1, 3, 4	13.88	15.10	16.76	18.31	20.64
ACC	Thr1, 3	26.51	26.77	27.10	27.47	26.70
UGG	Trp	9.76	9.28	8.69	8.01	7.03
UGA	Stop	0.31	0.27	0.23	0.17	0.19
UGU	Cys	4.23	3.97	3.64	3.24	2.76
UGC	Cys	5.29	5.06	4.77	4.35	3.81
UAG	Stop	0.00	0.00	0.00	0.00	0.00
UAA	Stop	2.77	3.02	3.38	3.65	4.18
UAU	Tyr1, 2	10.68	9.90	8.90	7.85	6.72
UAC	Tyr1, 2	16.20	16.41	16.71	16.90	16.52
UUG	Leu4, 5	6.63	6.22	5.72	4.93	4.27
UUA	Leu5	6.13	5.46	4.64	3.56	2.73
UUU	Phe	12.55	11.54	10.30	8.72	7.92
UUC	Phe	22.68	22.55	22.44	22.68	23.25
UCG	Ser1, 2	6.05	5.41	4.58	3.75	2.51
UCA	Ser1	3.89	3.54	3.09	2.55	1.98
UCU	Ser1, 5	13.12	13.54	14.14	14.84	16.33
UCC	Ser5	11.15	11.57	12.09	12.34	11.68
CGG	Arg3	1.75	1.52	1.23	0.90	0.62
CGA	Arg2	1.32	1.17	0.99	0.75	0.67
CGU	Arg2	31.12	33.46	36.61	39.60	43.82
CGC	Arg2	22.25	22.31	22.39	21.76	20.59
CAG	Gln2	29.24	28.80	28.33	27.69	27.28
CAA	Gln1	10.19	9.65	8.98	7.99	7.01
CAU	His	9.23	8.72	8.11	7.23	6.78
CAC	His	13.90	13.90	13.91	14.08	14.21
CUG	Leu1, 3	60.13	60.62	61.29	61.59	60.75
CUA	Leu3	2.15	1.87	1.53	1.09	0.82
CUU	Leu2	5.70	5.22	4.64	4.01	3.86
CUC	Leu2	6.19	5.91	5.52	5.03	4.09
CCG	Pro1, 3	29.51	29.22	28.88	28.91	28.82
CCA	Pro3	6.52	6.47	6.40	6.08	5.18
CCU	Pro2, 3	4.99	4.90	4.79	4.62	4.38
CCC	Pro2	3.32	2.77	2.10	1.40	1.09
AUG	Met f1, 2	2.95	3.16	3.48	3.69	4.23

The frequency of usage for all 61 sense codons and the three stop codons is calculated as described in the text using the data from Pedersen *et al*. (1978) and VanBogelen *et al*. (1992).

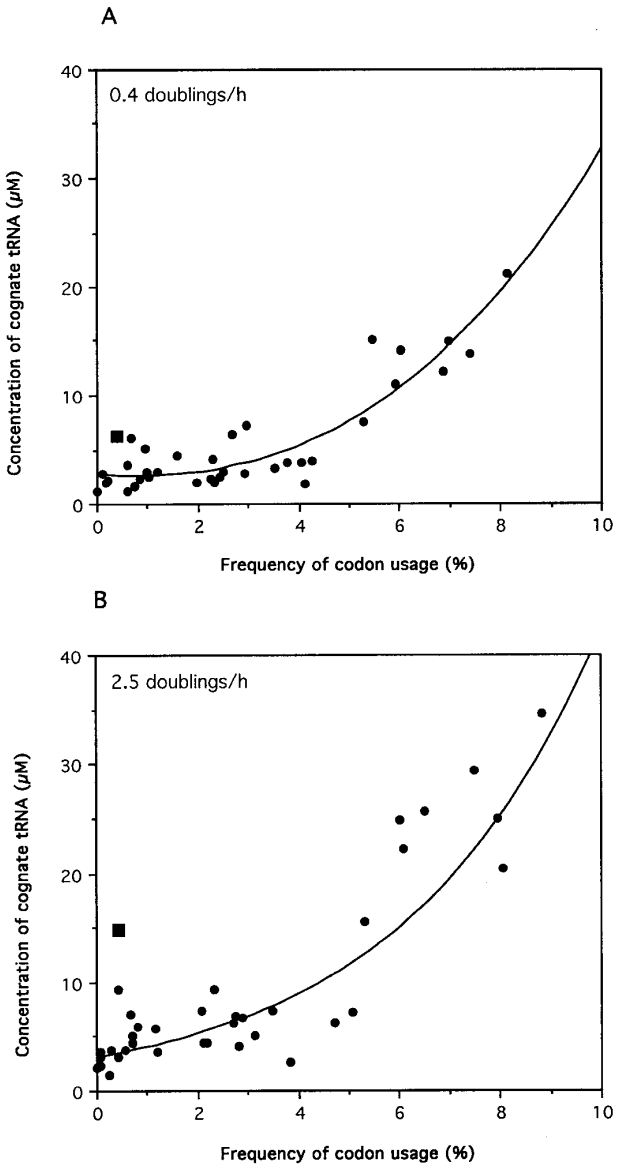

Figure 5. Correlations between the abundance of tRNA (μM) and the frequency of usage of the cognate codon. The intracellular concentrations of individual tRNAs are from Table 5 and the frequency of usage of the corresponding codons is from Table 4. Correlations are shown for the cell at the slowest (A) and fastest (B) growth rates, i.e. 0.4 and 2.5 doublings/hour, respectively. In the case of multiple codon recognitions by the same tRNA isoacceptor, a sum of all the cognate codon frequencies is plotted against the corresponding tRNA. In the case of a single codon recognized by more than one tRNA isoacceptor, the frequency of this particular codon is distributed among the tRNAs according to their relative abundance in cells. Reductant tRNAs (fMet 1 + 2, Val2A + 2B, Tyr1 + 2 or Thr1 + 3) are treated as a collective tRNA. (■) $tRNA_f^{Met}$. $tRNA^{Sel\text{-}Cys}$ (UGA) is omitted in this plot due to its particular codon recognition.

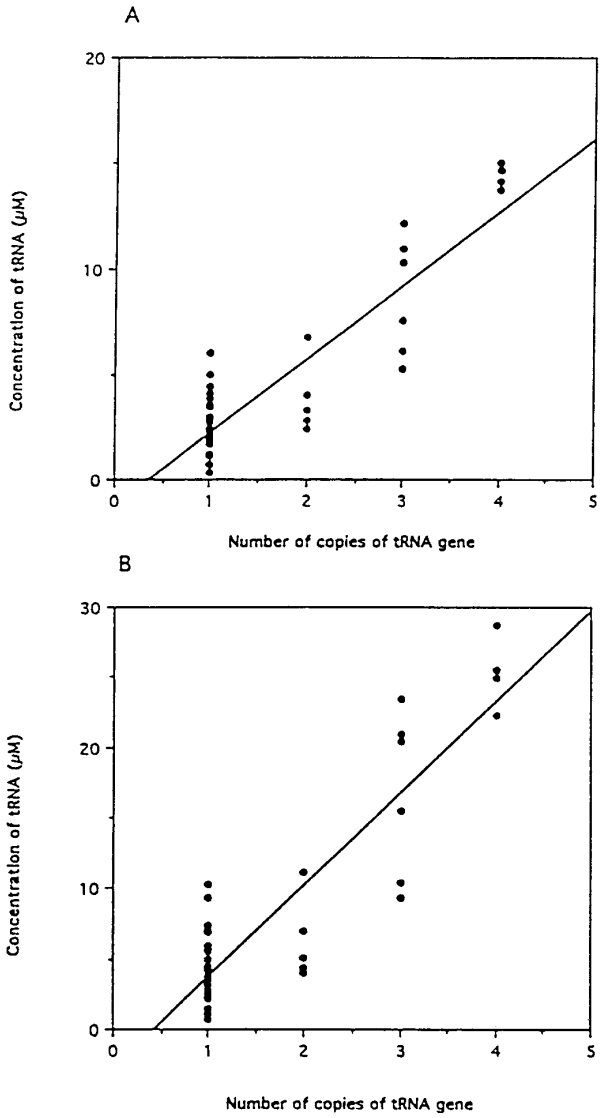

Figure 6. Correlations between the tRNA concentration (μM) and the copy numbers of the respective tRNA gene. The data represented here are: A, for bacteria cultivated at the slowest growth rate (0.4 doubling per hour); and B, for bacteria cultivated at the fastest growth rate (2.5 doublings per hour).

Kurland (1990) as well as of Emilsson *et al*. (1993), who measured the relative abundance of an overlapping set of 18 tRNA species in *E. coli*. However, the present data on growth rate-dependent variations of tRNA abundance disagree in important ways with the descriptions of the growth rate dependence of the tRNA abundance previously reported from this laboratory (Emilsson & Kurland, 1990; Emilsson *et al*., 1993).

For example, our earlier data suggested that the abundance of major tRNA species normalized to ribosomes remains relatively constant, whereas the abundance of most minor tRNA species relative to ribosomes decreases as growth rates are increased (Emilsson & Kurland, 1990; Emilsson *et al*., 1993). We also identified several minor tRNA species that seemed to increase in abundance relative to ribosomes with increasing growth rates (Emilsson & Kurland, 1990; Emilsson *et al*., 1993). In contrast,

the present data suggest that the abundance of all 46 tRNA species normalized to that of ribosomes decreases monotonically when the growth rate increases between 0.4 and 2.5 doublings per hour. Furthermore, the differences between the distributions of tRNAs at the fastest and at the slowest growth rates are much smaller than reported (Emilsson & Kurland, 1990; Emilsson *et al*., 1993).

There are a number of potential explanations for these discrepancies. One relevant detail is that the growth rates of bacteria in the M9-based media favoured earlier leads to a narrower growth rate range than that obtained in the MOPS media used here. This is illustrated by the growth rate range of 0.5 to 2.1 doublings/hour obtained earlier compared with the range in comparable media of 0.4 to 2.5 doublings/hour obtained here. Our choice of MOPS buffered media was motivated by the intention to use the protein abundance data obtained by Pedersen *et al*. (1978) and VanBogelen *et al*. (1992) in the same media.

Secondly, control experiments indicate that preferential loss of the big ribosomal RNA molecules (i.e. 16 S and 23 S rRNAs) occurs when too large an amount of bacterial mass is used in the phenol extraction of total RNA, as in the previous experiments (Emilsson & Kurland, 1990). We find that there is a more effective and reproducible recovery of ribosomal RNA when the bacterial mass to phenol volume is reduced by a factor of 10 compared to that used previously (Emilsson & Kurland, 1990). Likewise, we observe a selective loss in the transfer of the large ribosomal RNA molecules from a 1.2% agarose gel to a filter paper during three hours of trans-blotting that was used in the earlier assays (Emilsson & Kurland, 1990; Emilsson *et al*., 1993). Control experiments show that a minimum of six hours of trans-blotting is required for a complete transfer of 16 S rRNA or 23 S rRNA from the gel to the filter. In brief, our control experiments suggest that there may have been a systematic underestimation of the recovery of 16 S rRNA under the assay conditions favoured earlier (Emilsson & Kurland, 1990; Emilsson *et al*., 1993). Since many of the calculations presented in the previous studies were based on measurements of tRNA/16 S rRNA ratios, selective loss of ribosomal RNA very probably distorted the previous results, particularly at the highest growth rates.

We were also concerned about the exceptional behaviour of some of the minor tRNA species in the earlier experiments that we failed to observe here. Therefore, a number of control experiments were performed in order to check recoveries of tRNA species at all stages of our assay. For example, we determined the extent to which loss of material could be due to leakage of small tRNAs through the filter during the process of trans-blotting. Accordingly, we applied more than one filter to a two-dimensional polyacrylamide gel containing the fractionated radioactive tRNA samples. Subsequent trans-blotting was performed at room temperature overnight (more than 16 hours). We find that all tRNA material is blotted onto the first filter with no detectable radioactivity in the second and third filters. We also repeated measurements of the molar ratio of $tRNA_3^{Gly}$, $tRNA_2^{Leu}$, $tRNA_5^{Leu}$ and $tRNA_1^{Ser}$ to ribosome using a modified Northern blotting protocol as described in Materials and Methods. The results obtained for these randomly chosen tRNA isoacceptors were in excellent agreement with those obtained by recovery measurements from the two-dimensional gel system (Table 3).

Finally, we find that the present results obtained by measuring RNA recovery from the two-dimensional gel system are reproducible. We repeated all of the measurements at the slowest growth rates at least six times and the standard deviations of the results for each individual tRNA isoacceptor were calculated. We observe that the standard deviation varies from $\pm 5\%$ for the major tRNAs to between $\pm 10\%$ and $\pm 15\%$ for a majority of the less abundant tRNAs, while for two of the least abundant tRNA species, we obtain a standard deviation close to $\pm 30\%$ (Table 2).

Finally, if the previous results were distorted primarily by poor recoveries of ribosomal RNA at the fastest growth rates, where ribosomes are at their highest concentrations, results that were obtained in the earlier experiments independent of the ribosomal RNA normalizations should be in closer agreement with the present data. When we recalculate the tRNA measurements based on estimates of the major tRNA isoacceptor concentrations normalized to $tRNA_1^{Leu}$ using the data of Emilsson & Kurland (1990), they are in excellent agreement with the present data. The disagreements between the results obtained in the different studies for the minor tRNA species are probably due to the quantitative limitations of the Northern blot technique that was used previously (Emilsson & Kurland, 1990; Emilsson *et al*., 1993). Thus, these earlier estimates were based on standard titration curves with known amounts of pure tRNA species. Unlike the titration curves described above, these titration curves were not linear in the concentration range that was employed then. For this reason, we suspect that extrapolations from the distorted tritration curves led to errors in the estimates of tRNA abundance in the previous reports (Emilsson & Kurland, 1990; Emilsson *et al*., 1993).

Variation of RNA abundance

The most consistent tendency in our data is that all of the tRNA species in *E. coli* tend to decrease in abundance relative to ribosomal RNA as the growth rate increases (Table 3). The extent of the decrease is slightly greater for minor tRNA isoacceptors compared with that for major tRNA isoacceptors, but in general this difference is small. For example, there is roughly a 50% reduction in the ribosome normalized ratio of the major $tRNA_1^{Leu}$ and about a 70% decrease for the minor $tRNA_5^{Leu}$ as growth rates are increased from 0.4 to 2.5

Table 5. The intracellular concentration (μM) of tRNA isoacceptors as a function of growth rate (doublings/hour)

tRNA	0.4	0.7	1.07	1.6	2.5
Ala1B	10.25	11.73	14.06	17.52	20.97
Ala2	1.95	2.12	2.33	3.19	3.57
Arg2	15.00	14.54	15.54	23.77	25.57
Arg3	2.01	2.61	1.45	2.26	2.30
Arg4	2.74	2.35	2.64	3.26	3.52
Arg5	1.23	1.57	1.61	2.46	2.20
Asn	3.77	3.86	4.35	6.10	7.29
Asp1	7.56	8.13	8.42	12.04	15.46
Cys	5.01	4.88	5.23	7.04	7.07
Gln1	2.41	2.72	3.63	3.17	4.38
Gln2	2.78	3.08	3.47	5.07	6.27
Glu2	14.88	15.58	16.71	24.12	29.35
Gly1 + 2	6.75	7.18	7.74	10.95	11.08
Gly3	13.76	15.21	16.75	19.84	24.96
His	2.02	2.19	2.63	3.35	4.38
Ile1 + 2	10.96	11.85	13.24	18.92	24.74
Leu1	14.11	14.91	16.76	21.32	22.20
Leu2	2.97	3.47	4.04	4.72	5.93
Leu3	2.10	2.49	2.62	3.19	3.17
Leu4	6.04	6.33	6.97	9.66	9.30
Leu5	3.57	3.47	4.07	3.65	3.78
Lys	6.08	6.80	7.35	8.73	10.43
Met f1	3.82	4.82	6.01	6.33	10.22
Met f2	2.26	2.28	2.36	3.38	3.77
Met m	2.23	2.59	2.91	4.10	4.43
Phe	3.27	3.60	4.29	4.69	5.11
Pro1	2.84	2.44	3.51	2.75	2.67
Pro2	2.27	2.51	2.26	4.01	3.75
Pro3	1.83	1.89	2.22	2.55	2.56
Sel-Cys	0.69	0.86	0.96	1.05	1.04
Ser1	4.09	5.56	5.47	6.98	7.36
Ser2	1.09	1.04	1.17	1.37	1.45
Ser3	4.44	4.39	4.53	5.40	5.67
Ser5	2.41	2.60	2.87	3.68	4.03
Thr1	0.32	0.41	0.54	0.56	0.67
Thr2	1.71	2.00	2.11	2.67	3.12
Thr3	3.46	3.73	3.87	4.86	5.54
Thr4	2.89	3.17	3.25	4.99	6.89
Trp	2.98	2.78	3.35	4.15	5.02
Tyr1	2.43	2.41	2.70	4.61	4.19
Tyr2	3.98	3.86	3.75	5.22	5.04
Val1	12.12	12.07	11.07	18.99	20.39
Val2A	1.99	2.00	2.38	2.70	2.79
Val2B	2.00	2.39	2.64	3.61	4.42
4.5 S RNA	1.13	1.46	1.72	2.18	2.55

The intracellular concentration of tRNA (expressed as μM) was calculated from data for the number of ribosomes per cell at different growth rates (Bremer & Dennis, 1987), the volume of cells at different growth rates (Donachie & Robinson, 1987) and the data obtained here for the tRNA/ribosome ratios.

doublings/hour (Table 3). In addition, the sum of tRNAs normalized to ribosomes decreases by about 50% (Figure 3). Consequently there are roughly 13 tRNA molecules per ribosome in the bacteria growing at a rate of 0.4 doubling per hour, and this is reduced to roughly six tRNA molecules per ribosome at the growth rate of 2.5 doublings per hour (Figure 3). This result, which is based on the summation of the individual tRNA/ribosome ratios, is supported by an experiment in which the mass ratio of total tRNA/ribosomal RNA was measured at different growth rates. Thus, the data in Figure 4 show that the mass ratio of the unfractionated tRNA species to total ribosomal RNA decreases by 50% as the growth rates are increased from 0.4 to 2.5 doublings per hour.

It is worth emphasizing that the absolute concentration of total tRNA increases by nearly 80% in cells growing at 2.5 doublings per hour compared with those growing at 0.4 doubling per hour (see Table 5). The decrease in the tRNA/ribosome ratio arises because the absolute concentration of ribosomes increases by as much as 250%. Hence, the ratio of tRNA to ribosomes decreases by roughly 50%.

This result is consistent with the suggestion that there is an optimal arrangement for the translation components, which in turn dictates the maximal growth rate of bacteria in different media (Ehrenberg & Kurland, 1984). According to this model the optimal ratio of ternary complex (EF-Tu·GTP·aminoacyl-tRNA) is a variable of the growth rates (Ehrenberg & Kurland, 1984). Here, when growth rates are increased, the mass of tRNA and elongation factors normalized to that of the ribosomes should decrease as the absolute concentration of ribosomes increases. Such a variable arrangement of the mass investment in the different components of the translation apparatus is attended by two effects on the performance of the translation apparatus. One effect is associated with the increased concentration of all of the components of the system, and this is expressed as an increase in total rate of protein synthesis. The second effect follows from the decreasing ratio of the mass of tRNA plus elongation factors normalized to the mass of ribosomes. This decrease in the relative amount of biomass invested in tRNA and elongation factors improves the efficiency of translation because one of the costs of translation in the growing cell is the amount of biomass that must be produced and invested in the translation apparatus itself (Ehrenberg & Kurland, 1984). In effect, this sort of optimization requires that the translation system is both expanded and trimmed as growth rates increase so that the rates of protein synthesis per total mass of translation apparatus increase. This pattern has been verified for the elongation factors (Pedersen *et al*., 1978; Kurland, 1993), and now it has been verified for the tRNAs in the present study.

Co-variation of tRNA abundance and codon usage

Another aspect of an optimal arrangement for the translation system is that the distribution of individual tRNA species should be a positive function of the cognate codon frequencies (Garel, 1974; von Heijne & Blomberg, 1979; Ehrenberg & Kurland, 1984). Plots of the individual tRNA concentrations as a function of the frequency of usage for the respective codons show that there is a positive correlation between these parameters at all growth rates (Figure 5). Thus, the amounts of the individual tRNAs accumulated at the different bacterial growth rates change, but they do so in a

way that is correlated with the changes in their cognate codon frequencies. In particular, the tRNA species present in relatively higher concentrations at the slowest growth rates are cognate to the most abundant codons used at these growth rates, while the tRNA isoacceptors present in lower concentrations are cognate to the rarer codons (Figure 5, Table 5). As the growth rates increase, the relative investment in the major tRNAs increases along with the corresponding cognate codon usage. As a consequence, the distributions of tRNAs along with their cognate codons become more extremely skewed as the growth rates increase.

These tendencies are expected because the protein population is progressively more dominated by a subset of proteins, such as the ribosomal proteins and the elongation factors EF-Tu and EF-G, as the growth rates increase. Since this subset of proteins is coded by a biased distribution of codons, the most efficient translation system would reflect this codon bias in a correspondingly biased tRNA abundance (Ehrenberg & Kurland, 1984; Kurland, 1993).

Nevertheless, there is a very big problem here. We would expect that the variation of tRNA concentrations would follow the square root of the corresponding cognate codon frequencies (Garel, 1974; von Heijne & Blomberg, 1979; Ehrenberg & Kurland, 1984). This is most certainly not observed because the individual tRNA abundance seems to vary as the square of the cognate codon frequency (Figure 5). There could be a number of reasons for this quantitative discrepancy.

First, the kinetics of translation are most clearly related to the free concentrations of ternary complex rather than to the total concentration of the tRNAs in the bacterium (Ehrenberg & Kurland, 1984). Therefore, it is the free ternary complex, and not the total tRNA, that should be correlated with the codon usage. We assume for simplicity that all of the tRNA that is not bound to the translating ribosomes is in the form of free ternary complex. We also take into consideration the data suggesting that approximately 80% of the ribosomes are actively engaged in translation elongation at any time, independent of the growth rate (Forchhammer & Lindahl, 1971). Since there are two tRNA molecules that are simultaneously bound on each ribosome (Nierhaus, 1990; Noller, 1991), the concentration of individual tRNA species bound by the ribosome will be determined by the ribosome-bound cognate codon frequency times twice the elongating ribosome concentration. When the total tRNA data are corrected accordingly for the amounts of tRNA bound to ribosomes, the correlation between the free ternary complex concentrations as a function of the corresponding codon frequencies is not very different from the correlations observed in Figure 5 (data not shown).

There are other details that can influence the forms of these correlations. One is that the rate constants describing the acquisition of ternary complex by codon-programmed ribosomes may vary for different pairs of tRNAs and their cognate codons. An important assumption of the optimization equations is that the rate constants describing the association of the different tRNA–codon pairs on the ribosome are the same (Garel, 1974; von Heijne & Blomberg, 1979; Ehrenberg & Kurland, 1984). They are almost certainly not the same (Curran & Yarus, 1989). Another complication is provided by the fact that there are tRNAs that translate more than one codon, and there are codons that are translated by more than one tRNA. Both sorts of degeneracy somewhat complicate the equations correlating optimal tRNA abundance with codon frequencies. Finally, a fundamental biological assumption upon which the optimization equations are based is that competition by growth rate is the only selective condition imposed on the optimization system (Ehrenberg & Kurland, 1984). There are strong indications that this assumption is incorrect for natural populations (Mikkola & Kurland, 1991, 1992). The influences of these different parameters on the tRNA–codon correlations will be discussed in detail elsewhere (Berg & Kurland, unpublished results).

Finally, the initiator $tRNA_f^{Met}$ provides striking exceptions to these correlations. Thus, this particular tRNA species increases in abundance with the growth rate to a much greater degree than the increase in the frequency of usage for the initiation codon AUG at the faster growth rates (Figure 5, Tables 4 and 5). The selectively higher concentrations of the initiator $tRNA_f^{Met}$ in fast growing cells may reflect a functional requirement for a particularly rapid mobilization of 30 S ribosome subunits during initiation under faster growth conditions.

Control of tRNA abundance

The growth rate-dependent variations of individual tRNA concentrations as well as their tendency to follow their cognate codon frequencies must reflect the workings of a rather elaborate physiological network that modulates the accumulation of the individual tRNAs. The observed correlation of tRNA concentrations with gene dose (Figure 6) confirms the suggestion that gene dose influences the concentration of the tRNAs (Ikemura, 1981). Nevertheless, it is difficult to understand how gene dose effects can account completely for the growth rate-dependent aspect of the tRNA abundance.

There is a tendency for tRNAs coded by the same operon to be regulated similarly (Emilsson *et al*., 1993). Nevertheless, there are three tRNA isoacceptors, namely $tRNA_5^{Leu}$, $tRNA_3^{Arg}$ and $tRNA_3^{Ser}$, the concentrations of which remain relatively unchanged while other tRNA species in common operons (Komine *et al*., 1990) increase in concentration with the growth rate (Table 5). Nevertheless, the abundance of these three minor tRNA isoacceptors changes co-ordinately with variations in the respective codon usage. Therefore, there may be other regulatory mechanisms, besides those

modulating co-transcription from the same promoter, that regulate the expression of these three tRNA species. There is also evidence that genes close to the origin of chromosome replication tend to have higher expression levels than genes that are close to the termination site of replication (Condon *et al*., 1992). However, a close comparison of the present data for tRNA abundance and the chromosomal loci for tRNA genes in *E. coli* (Komine *et al*., 1990) did not reveal a systematic pattern.

Finally, we have tried to develop an experimental system to study the co-variation of tRNA abundance and codon usage by manipulating the codon composition of the mRNA pools (Dong *et al*., 1995). This attempt failed because bacteria die when their mRNA pools are distorted to a significant extent. Thus, the mechanisms that support a growth rate-dependent covariation of tRNA abundance and codon usage remain a mystery.

Materials and Methods

The strain and growth media

The bacterial strain used in this work is W1485, a derivative of *Escherichia coli* K12 (Emilsson & Kurland, 1990). The media were the defined MOPS as described by Neidhardt *et al*. (1977) with the following supplements: (1) 0.4% (w / v) sodium acetate; (2) 0.4% (w / v) sodium succinate; (3) 0.4% (w / v) glucose (w / v); (4) 0.4% (w / v) glucose plus ten amino acids (arginine, histidine, glycine, isoleucine, leucine, methionine, phenylalanine, serine, threonine and valine; Neidhardt *et al*., 1977); or (5) 0.4% (w / v) glucose plus 20 amino acids, vitamin B1, and four nucleic acid bases (adenine, cytosine, thymine and xanthine; Neidhardt *et al*., 1977). In addition, a low-phosphate MOPS / acetate medium was used for ^{32}P labelling; it contains 0.26 mM K_2HPO_4. Cells were grown aerobically in a 37°C water-bath with vigorous shaking. Under these conditions, *E. coli* W1485 grows in the five media listed above at rates of 0.4, 0.7, 1.07, 1.6, and 2.5 doublings per hour, respectively.

Preparation of total RNA

A 2 ml sample of cells from an exponential bacterial culture at a cell density corresponding to an A_{540} of 0.5 was pelleted and resuspended in 100 µl lysis buffer (25 mM Tris-HCl (pH 7.5), 60 mM KCl, 10 mM $MgCl_2$ and 4 mg / ml lysozyme). The cells were lysed by first freezing in solid CO_2 ethanol bath and then thawing in a 45°C water-bath for four consecutive repeats. Total RNA was extracted with phenol (pH 8.0) once and the interphase was extracted once again by adding 100 µl lysis buffer to the phenol layer. The aqueous phases from the two extractions with phenol were combined and used for total RNA precipitation using 2.5 volumes of 95% ethanol at –80°C for 12 hours. The RNA was dissolved in 20 µl 1 M Tris-HCl (pH 9.0) and incubated at 37°C for 30 minutes in order to deacylate tRNAs.

Fractionation and identification of tRNA on a two-dimensional polyacrylamide gel

The fractionation of tRNA was performed using two-dimensional polyacrylamide gel electrophoresis with a 10% (w / v) polyacrylamide gel containing 7 M urea in the first dimension (200 mm × 400 mm × 1 mm) and a 20% (w / v) polyacrylamide gel containing 4 M urea in the second (150 mm × 185 mm × 1 mm); both gels were made in 1 × TBE (Sambrook *et al*., 1989). The acrylamide used here is the premixed solution of acrylamide / bisacrylamide 19:1 (w / v); Ampligene). About 5 to 10 µg RNA in 10 µl of 1 M Tris-HCl (pH 9.0) as mixed with 10 µl formamide. The sample was incubated in a 60°C water-bath for five minutes and immediately chilled on ice for ten minutes before applying (20 µl in total) to the first-dimensional gel that has been prerun in 1 × TBE at 200 V for three hours in a 4°C room. The gel was electrophoresed at 350 V for 47 hours at 4°C. After electrophoresis, the gels were briefly stained with ethidium bromide in 1 × TBE buffer for one minute. The gel slice (about 14 cm in length and 0.5 cm in width) containing only 4 S RNA was cut out after identification with the aid of UV light and moulded on to the second-dimensional gels after a 90° rotation (Figure 1). The gel slice was sealed to the second-dimensional gel using 20% (w / v) polyacrylamide plus 4 M urea followed by electrophoresis at 220 V for 47 hours at room temperature.

The second-dimension gel was stained with ethidium bromide solution in 1 × TBE buffer. The individual tRNA spots were marked on the gel by making a tiny hole in the centre of each tRNA spot in the gel. Then the gel was laid onto a Hybond-N^+ filter (Amersham) that had been prewetted in 25 mM sodium phosphate buffer (pH 6.5). The tRNA spots were marked on the filter using a waterproof pen with the aid of the ''hole'' marker made in the gel. After trans-blotting in 25 mM sodium phosphate buffer (pH 6.5) for 12 hours, the filter was dried, UV-cross-linked and used as a master-filter for determination of the tRNA identity for each individual tRNA spot on the two-dimensional polyacrylamide gel.

The identity of each tRNA spot on the two-dimensional polyacrylamide gel was determined by hybridization of the master-filter with specific oligonucleotide probes (Table 1) that were end-labelled with [γ-^{32}P]ATP (Sambrook *et al*., 1989). In addition, the tRNA spots were individually cut out from the gel and trans-blotted onto a Hybond-N^+ filter. This filter was UV-cross-linked and hybridized with the oligonucleotide probe specific for each tRNA isoacceptor, to confirm the identity of tRNA spots and to be sure that each tRNA spot was hybridizing only with its specific oligonucleotide probe.

Quantification of the tRNA content in the cell

Exponentially growing cells of *E. coli* W1485 in each of the five media listed above were uniformly labelled for two generations (300, 170, 112, 75, and 48 minutes, respectively) with 50 µCi of [5,6-^3H]uridine per ml (specific activity, 38 Ci / mmol; Amersham) in the presence of 10 µM non-radioactive uridine. In addition, an exponential culture of W1485 in a low-phosphate MOPS / acetate medium were uniformly labelled with 1 mCi ^{32}P per ml (carrier-free, Amersham) for 300 minutes. These cells are used as reference cells. Samples (1 ml) of cells labelled with [5,6-^3H]uridine in different growth media were each mixed with 1 ml of the reference cells. RNA (5 µg) corresponding to 2×10^6 cpm was used for the fractionation of individual tRNA species on two-dimensional polyacrylamide gels. After electrophoresis, the RNA fractionated on the two-dimensional gels was transferred on to a Hybond-N^+ filter (Amersham).

The filter was dried and autoradiographed for one to three hours at –80°C.

The individual tRNA spots were excised from the two-dimensional gel, and their isotope content was measured in a scintillation solution (Quickszint 701, Zinsser Analytical). Bits of gel that were devoid of RNA were excised, and their isotope content was used to estimate background isotope levels. In general, the background levels were 100 cpm or less; while the isotope content of tRNA spots varied from roughly 4000 cpm above background for major tRNA species to roughly 400 cpm above background for minor tRNA species. For two of the least abundant species, the isoacceptors corresponding to Sel-Cys and Thr1, the isotope contents were as low as 200 cpm over background. After correcting for the background radioactivity, the relative amounts of individual tRNA isoacceptors at each growth rate were calculated by normalizing the isotope ratio of $^{3}H/^{32}P$ in each tRNA spot to that in the spot corresponding to $tRNA_1^{Leu}$.

The relative amount of each tRNA species normalized to that of $tRNA_1^{Leu}$ at the lowest growth rate was used as a standard for comparison of the same ratios at the other growth rates. This ratio for all the tRNA species at the lowest growth rate was determined as follows; an exponentially growing cells of W1485 in the MOPS/acetate medium was uniformly labelled with 5 μCi [U-^{14}C]uridine per ml (specific activity, 50 μCi/ml) for two generations (300 minutes). Total RNA preparation from 2 ml of the ^{14}C-labelled cells, fractionation of tRNAs on two-dimensional gels and quantification of the tRNA spots are as described above except that the autoradiography was carried out at –80°C for about 7 to 14 days. The molar amount of each tRNA relative to that of $tRNA_1^{Leu}$ was measured by normalizing the amount of the radioactivity in the respective tRNA spot to that in the spot of $tRNA_1^{Leu}$, after correction for a small difference in the number of U nucleotides that they contain. Then the fraction of each tRNA out of total tRNA was calculated by normalizing the amount of radioactive content in each tRNA spot to the sum of the radioactive content in all tRNA spots.

Determination of the cellular concentration of $tRNA_1^{Leu}$

The amount of $tRNA_1^{Leu}$ accumulated in the cell was determined as follows. Aliquots of total RNA prepared as above (about 3 μg in 10 μl of 1 M Tris-HCl (pH 9.0)) were mixed with 10 μl of formamide. The samples were incubated in a 60°C water-bath for five minutes and chilled on ice for ten minutes before they were applied to a 1.2% (w/v) agarose/formaldehyde gel (Dong *et al*., 1995). In addition, the pure ribosomal RNA (23 S, 16 S and 5 S) (purified from *E. coli* 70 S ribosomes) and the pure $tRNA_1^{Leu}$ (purified from two-dimensional polyacrylamide gels) were applied to the same agarose gel in varying amounts. After electrophoresis, RNA including the rRNA and $tRNA_1^{Leu}$ standards were trans-blotted on to a Hybond-N$^+$ filter (Amersham). The filter was hybridized with excess amount of two specific oligonucleotide probes, one of which corresponds to 16 S rRNA and the other to $tRNA_1^{Leu}$. The molar amount of $tRNA_1^{Leu}$ relative to that of 16 S rRNA at different growth rates was obtained by comparison of the amounts of probe that hybridize to the different electrophoretic components in the experimental samples and in the titration curves obtained for the pure rRNA and $tRNA_1^{Leu}$ standards (Figure 2).

Measurements of the mass ratio of tRNA/rRNA

Exponentially growing cells were uniformly labelled with [5,6-^{3}H]uridine for two generations as described above. The RNA lysates were prepared and fractionated on a 1.2% (w/v) agarose/formaldehyde gel (Dong *et al*., 1995). The gel was stained with ethidium bromide. The RNA bands corresponding to 23 S and 16 S rRNA and total tRNA (this band contains 5 S rRNA) were excised from the gel with the aid of UV light. Treatments of the gel slices for counting of their isotope contents were described (Dong *et al*., 1995). The fraction of the isotope content corresponding to 5 S rRNA was calculated on the assumption of a 1:1:1 molar ratio between 23 S:16 S:5 S rRNAs in the cell (Bremer & Dennis, 1987) and subtracted from the isotope content in the total tRNA band. The mass ratio of tRNA/rRNA is defined as the amount of radioactivity (counts per minute) in total tRNA normalized to that in total rRNA (23 S + 16 S + 5 S).

Calculation of codon usage at different growth rates

The growth rate-dependent variation in abundance of 140 different proteins has been studied in *Escherichia coli* (Pedersen *et al*., 1978). These 140 individual proteins are divided into five groups according to their characteristic behaviour in response to growth rate variations. The proteins in group Ia decrease in abundance, the proteins in group Ib remain relatively constant, and the proteins in group Ic increase in abundance with increasing growth rate. The proteins in groups IIa and IIb show a variable response to growth rate variations (Pedersen *et al*., 1978). The sum of these 140 proteins in combination with 50 additional ribosomal proteins accounts for two-thirds of the protein mass of the bacteria (Pedersen *et al*., 1978).

In order to calculate the frequency of usage for all 61 sense codons as a function of the growth rate, the identity for most of the proteins in each subgroup were deduced from two-dimensional protein database (VanBogelen *et al*., 1992). The corresponding coding sequences are retrievable from the Genbank, and the codon usage analysis was carried out with the CODONFREQUENCY program from the UWGCG package. Then, the average frequency of codon usage for each individual subgroup was calculated on the assumption that the amount of a particular protein accumulated in the cell during the steady-state growth is proportional to the amount of the corresponding messenger RNA in the bacteria. Finally, the average frequency of usage for each individual codon for each growth rate is computed on the basis of the relative weight fraction of each protein group as determined by Pedersen *et al*. (1978). In this calculation, the initiation codon AUG is treated separately from the elongation codon AUG.

Acknowledgements

We thank Siv Andersson for comments on the manuscript. This work was supported by the Swedish

Cancer Society and the Natural Sciences Research Council.

References

Björk, G. R. (1995). Biosynthesis and function of modified nucleotides. In *tRNA: Structure, Biosynthesis, and Function* (Söll, D. & RajBhandary, U. L., eds), pp. 165–205, American Society for Microbiology, Washington, DC 20005.

Bremer, H. & Dennis, P. P. (1987). Modulation of chemical composition and other parameters of the cell by growth rate. In Escherichia coli *and* Salmonella typhimurium (VanBogelen, F. C., Ingraham, J. L., Low, K. B., Magasanik, B., Schaechter, M. & Umbarger, H. E., eds), pp. 1527–1542, American Society for Microbiology, Washington, DC.

Condon, C., Philips, J., Fu, Z.-Y., Squires, C. & Squires, C. L. (1992). Comparison of the expression of the seven ribosomal RNA operons in *Escherichia coli*. *EMBO J.* **11**, 4175–4185.

Curran, J. F. & Yarus, M. (1989). Rates of aminoacyl-tRNA selection at 29 sense codons *in vivo*. *J. Mol. Biol.* **209**, 65–77.

Donachie, W. D. & Robinson, A. C. (1987). Cell division: parameter values and the process. In Escherichia coli *and* Salmonella typhimurium (VanBogelen, F. C., Ingraham, J. L., Low, K. B., Magasanik, B., Schaechter, M. & Umbarger, H. E., eds), pp. 1578–1593, American Society for Microbiology, Washington, DC.

Dong, H., Nilsson, L. & Kurland, C. G. (1995). Gratuitous overexpression of genes in *Escherichia coli* leads to growth inhibition and ribosome destruction. *J. Bacteriol.* **177**, 1497–1504.

Ehrenberg, M. & Kurland, C. G. (1984). Cost of accuracy determined by a maximal growth rate constraint. *Quart. Rev. Biophys.* **17**, 45–82.

Emilsson, V. & Kurland, C. G. (1990). Growth rate dependence of transfer RNA abundance in *Escherichia coli*. *EMBO J.* **9**, 4359–4366.

Emilsson, V. & Nilsson, L. (1995). Factor for inversion stimulation-dependent growth rate regulation of serine and threonine tRNA species. *J. Biol. Chem.* **270**, 16610–16614.

Emilsson, V., Näslund, A. K. & Kurland, C. G. (1993). Growth rate dependent accumulation of 12 tRNA species in *Escherichia coli*. *J. Mol. Biol.* **230**, 483–491.

Forchhammer, J. & Lindahl, L. (1971). Growth rate of polypeptide chains as a function of the cell growth rate in a mutant of *Escherichia coli* 15. *J. Mol. Biol.* **55**, 563–568.

Garcia, G. M., Mar, P. K., Mullin, D. A., Walker, J. R. & Prather, N. E. (1986). The *E. coli dnaY* gene encodes an arginine transfer RNA. *Cell*, **45**, 453–459.

Garel, J. P. (1974). Functional adaptation of tRNA population. *J. Theoret. Biol.* **43**, 211–225.

Ikemura, T. (1981). Correlation between the abundance of *Escherichia coli* transfer RNAs and the occurrence of the respective codons in its protein genes. *J. Mol. Biol.* **146**, 1–21.

Ikemura, T. (1985). Codon usage and tRNA content in unicellular and multicellular organisms. *Mol. Biol. Evol.* **2**, 13–34.

Ikemura, T. & Ozeki, T. (1983). Codon usage and transfer RNA contents: organism-specific codon-choice patterns in reference to the isoacceptor contents. *Cold Spring Harbor Symp. Quant. Biol.* **47**, 1083–1097.

Komine, Y., Adachi, T., Inokuchi, H. & Ozeki, H. (1990). Genomic organization and physical mapping of the transfer RNA genes in *Escherichia coli* K12. *J. Mol. Biol.* **212**, 579–598.

Kurland, C. G. (1993). Major codon preference: theme and variations. *Biochem. Soc. Trans.* **21**, 841–846.

Mikkola, R. & Kurland, C. G. (1991). Is there a unique ribosome phenotype for naturally occuring *Escherichia coli*? *Biochimie*, **73**, 1061–1066.

Mikkola, R. & Kurland, C. G. (1992). Selection of laboratory wildtype phenotype from natural isolates of *E. coli* in chemostats. *Mol. Biol. Evol.* **9**, 394–402.

Neidhardt, F. C., Bloch, P. L., Pedersen, S. & Reeh, S. (1977). Chemical measurement of steady-state levels of ten aminoacyl-transfer ribonucleic acid synthetases in *Escherichia coli*. *J. Bacteriol.* **129**, 378–387.

Nierhaus, K. H. (1990). The allosteric three-site model for the ribosomal elongation cycle: features and future. *Biochemistry*, **29**, 4997–5007.

Noller, H. F. (1991). Ribosomal RNA and translation. *Annu. Rev. Biochem.* **60**, 191–227.

Pedersen, S., Bloch, P. L., Reeh, S. & VanBogelen, F. C. (1978). Patterns of protein synthesis in *E. coli*: a catalog of the amount of 140 individual proteins at different growth rates. *Cell*, **14**, 179–190.

Sambrook, J., Fritsch, E. F. & Maniatis, T. (1989). *Molecular Cloning: A Laboratory Manual*, 2nd edit., Cold Spring Harbor Laboratory Press, Cold Spring Harbor, NY.

Saxena, P. & Walker, J. R. (1992). Expression of *argU*, the *Escherichia coli* gene coding for a rare arginine tRNA. *J. Bacteriol.* **174**, 1956–1964.

VanBogelen, R. A., Sankar, P., Clark, R, L., Bogan, J. A. & Neidhardt, F. C. (1992). The gene–protein database of *Escherichia coli*: edit. 5. *Electrophoresis*, **13**, 1014–1054.

Von Heijne, G. & Blomberg, C. (1979). The concentration dependence of the error frequencies and some related quantities in protein synthesis. *J. Theoret. Biol.* **78**, 113–120.

Edited by J. Karn

(Received 8 January 1996; received in revised form 3 May 1996; accepted 15 May 1996)